Signature: © Pol J Radiol, 2012; 77(1): 37-46

Polish Journal of Radiology
www.PolRadiol.com

REVIEW ARTICLE

Received: 2011.12.15
Accepted: 2012.01.19

Ventilation and perfusion magnetic resonance imaging of the lung

Grzegorz Bauman[1], Monika Eichinger[2]

[1] German Cancer Research Center, Department of Medical Physics in Radiology, Heidelberg, Germany
[2] German Cancer Research Center, Department of Radiology, Heidelberg, Germany

Author's address: Grzegorz Bauman, Research Scientist, German Cancer Research Center, Project Group – Perfusion MRI, Department of Medical Physics in Radiology Im Neuenheimer Feld 280, 69120 Heidelberg, Germany, e-mail: g.bauman@dkfz.de

Summary

A close interaction between the respiratory pump, pulmonary parenchyma and blood circulation is essential for a normal lung function. Many pulmonary diseases present, especially in their initial phase, a variable regional impairment of ventilation and perfusion. In the last decades various techniques have been established to measure the lung function. Besides the global pulmonary function tests (PFTs) imaging techniques gained increasing importance to detect local variations in lung function, especially for ventilation and perfusion assessment. Imaging modalities allow for a deeper regional insight into pathophysiological processes and enable improved planning of invasive procedures. In contrast to computed tomography (CT) and the nuclear medicine techniques, magnetic resonance imaging (MRI), as a radiation free imaging modality gained increasing importance since the early 1990 for the assessment of pulmonary function. The major inherent problems of lung tissue, namely the low proton density and the pulmonary and cardiac motion, were overcome in the last years by a constant progress in MR technology. Some MR techniques are still under development, a process which is driven by scientific questions regarding the physiology and pathophysiology of pulmonary diseases, as well as by the need for fast and robust clinically applicable imaging techniques as safe therapy monitoring tools. MRI can be considered a promising ionizing-free alternative to techniques like CT or nuclear medicine techniques for the evaluation of lung function. The goal of this article is to provide an overview on selected MRI techniques for the assessment of pulmonary ventilation and perfusion.

Key words: lung • function • magnetic resonance imaging

PDF file: http://www.polradiol.com/fulltxt.php?ICID=882579

Background

Lung function is the result of a close interaction between the respiratory pump, lung parenchyma and pulmonary circulation. As diseases of the respiratory system can affect each of these components, a clear differentiation between the individual contributors to a functional impairment is essential for adequate diagnostics and treatment. Many pulmonary diseases, especially in their initial phase, present a variable regional involvement of ventilation and perfusion. Thus, mismatch between these two components may occur.

In the last decades various techniques have been established to measure the lung function. Pulmonary function tests (PFTs) including spirometry and body plethysmography remain the main tools for measurements of lung volumes, air-flow and resistance [1]. For better disease characterization they can be used in combination with other procedures such as arterial blood gas partial pressure analysis, breathing gas analysis, carbon monoxide diffusion capacity. However, all these methods provide only global parameters of lung function, therefore are often nonspecific to differentiate lung diseases, or not sensitive enough to detect early functional lung damage, especially in case of heterogeneous ventilation and perfusion abnormalities [2]. Moreover, it is difficult to perform PTFs in young children because the measured parameters are dependent upon the patient's compliance, e.g. their ability to perform the appropriate maneuver properly. A more powerful method

to analyze pulmonary gas exchange is the multiple inert gas elimination technique (MIGET) [3], which allows for partial assessment of lung heterogeneity and determination of ventilation-perfusion ratio. This is possible by measuring the mixed arterial, venous, and expired concentrations of six infused inert gases [4]. The main limitations of MIGET are high technical demand, invasiveness and analysis based on complex mathematical models.

Another possibility to measure ventilation inhomogeneity is the multiple breath wash out method (MBW). This method is based on the inhalation of inert gases, in the majority of cases sulfur hexafluoride (SF_6) together with a mixture of helium, nitrogen and oxygen in a specific concentration. The exhaled gas concentrations are measured at the mouth either by mass spectrometry [5] or by mainstream ultrasonic flow sensors [6] and a lung clearance index (LCI) is calculated. Although LCI is able to determine early ventilation inhomogeneities in the human lung, its use is limited due to the lack of commercially available equipment and the demanding accomplishment of the procedure and interpretation of data [7].

For the aforementioned reasons, imaging techniques are of particular interest to detect regional variations in lung function. Imaging modalities allow for a deeper regional insight into pathophysiological processes and enable improved planning of invasive procedures as well as non-invasive monitoring of therapeutic response. The conventional chest radiography is traditionally used to monitor lung structure, yet it provides no functional information. In clinical routine imaging of the lung function has been primarily restricted to methods based on the application of radioactive labeled tracers, such as planar scintigraphy [8] and single photon emission computed tomography (SPECT) [9], the latter providing three-dimensional images. Ventilation measurement is performed by inhalation of ^{99,m}Tc-Technegas, ^{127}Xe or ^{133}Xe, and perfusion by intravenous administration of ^{99,m}Tc macroaggregated albumin. The ventilation/perfusion ratio can be studied also using the positron emission tomography (PET) [10]. Besides harmful exposure of patients to ionizing radiation and time consuming examinations, nuclear imaging modalities have a relatively low spatial resolution and poor signal-to-noise ratio, which may lead to inconclusive diagnosis in case of subtle changes in lung function. Additionally, as they provide only static information there is no possibility to track fast physiological processes. Computer tomography (CT) and CT angiography have been established as routine clinical tools for assessment of lung parenchyma and blood vessels structure. In the last years dual-energy xenon- or iodine-enhanced computed tomography (CT) have been intensively investigated for ventilation and perfusion measurements [11,12]. For CT the most important advantages are high spatial resolution with short-examination times. However, high spatial resolution obtained by CT and especially when using ventilation-perfusion CT, is unfortunately associated with a relevant radiation exposure and limits its value for repetitive follow-up examinations in young adults, children, or pregnant women [13,14].

In contrast to CT and the nuclear medicine techniques, magnetic resonance imaging (MRI), a radiation free imaging modality, relies on magnetic properties of atoms possessing spin e.g. hydrogen contained in water or organic molecules in body tissues. MRI uses a strong magnetic field to measure signal induced with radio frequency waves of rotating magnetic moments. Thus, repeated or time-resolved measurements of lung dynamics are harmless for patients, if an allowed specific absorption rate is not exceeded. This fact opened the possibility to develop a broad spectrum of techniques in the last years providing information regarding different aspects of the pulmonary physiology and pathophysiology. Various parameters obtained with these techniques are used to analyze global lung function such as inspiratory or expiratory lung volumes [15], two- or three-dimensional respiratory dynamics [16,17], or regional lung function such as measurements of ventilation, pulmonary perfusion and diffusion. For the clinical application of lung MRI general contraindications (metallic implants, cardiac pacemaker) are valid. Another limiting factor for MRI is of economic nature and related to relatively high costs of examinations as well as the access problem especially to more sophisticated techniques requiring dedicated hardware or trained personnel. Hence, simple and easily implementable MRI based techniques are highly desirable. It is the goal of this article to provide an overview of selected MRI techniques for the assessment of the lung ventilation and perfusion.

Challenges of Lung MRI

Chest MRI as a radiation-free alternative has been explored since the 1990s [18]. It was successfully applied for diagnosis of mediastinal tumors, chest wall masses, or cardiac and large vessel imaging [19,20]. Initially lung parenchyma was not possible to be visualized using MRI. A constant progress in MR technology has also increased the value of this modality for pulmonary parenchymal imaging. Nevertheless, there are several technical and methodological reasons why studying of morphology and function of the lung using MRI is challenging. The major problem is associated with the unique foam like structure of the pulmonary parenchyma in a weight of approximately 1 kg distributed over a volume of 4 to 6 liters. Predominance of air within the pulmonary tissue implies a very low proton density in comparison to other parts of the body. Furthermore, the density of the lung decreases with age [21]. A large number of air-tissue and air-liquid interfaces in lung alveoli leads to local field inhomogeneities, which induces high susceptibility differences on intra-voxel scales responsible for phase dispersion of spins and rapid signal loss. Susceptibility effects are dominant on MR systems with increasing magnetic field strength. On a standard clinical 1.5T MR-scanner the effective transverse relaxation time T_2^* in lung parenchyma is extremely short of about 1–2 ms, the transverse relaxation time T_2 is in range of 30–80 ms and influenced by significant molecular diffusion [22]. On the other hand, the longitudinal relaxation time T_1 of 1100 to 1500 ms is relatively long [23]. Thus, going to higher magnetic field strengths in this case is problematic but possible [24]. The second problem of lung imaging is the continuous motion of all surrounding anatomical structures induced by pulsation of vessels, cardiac motion, but first of all by the respiratory movement.

In order to overcome these restrictions, new MR pulse sequences were developed and optimized for morphological

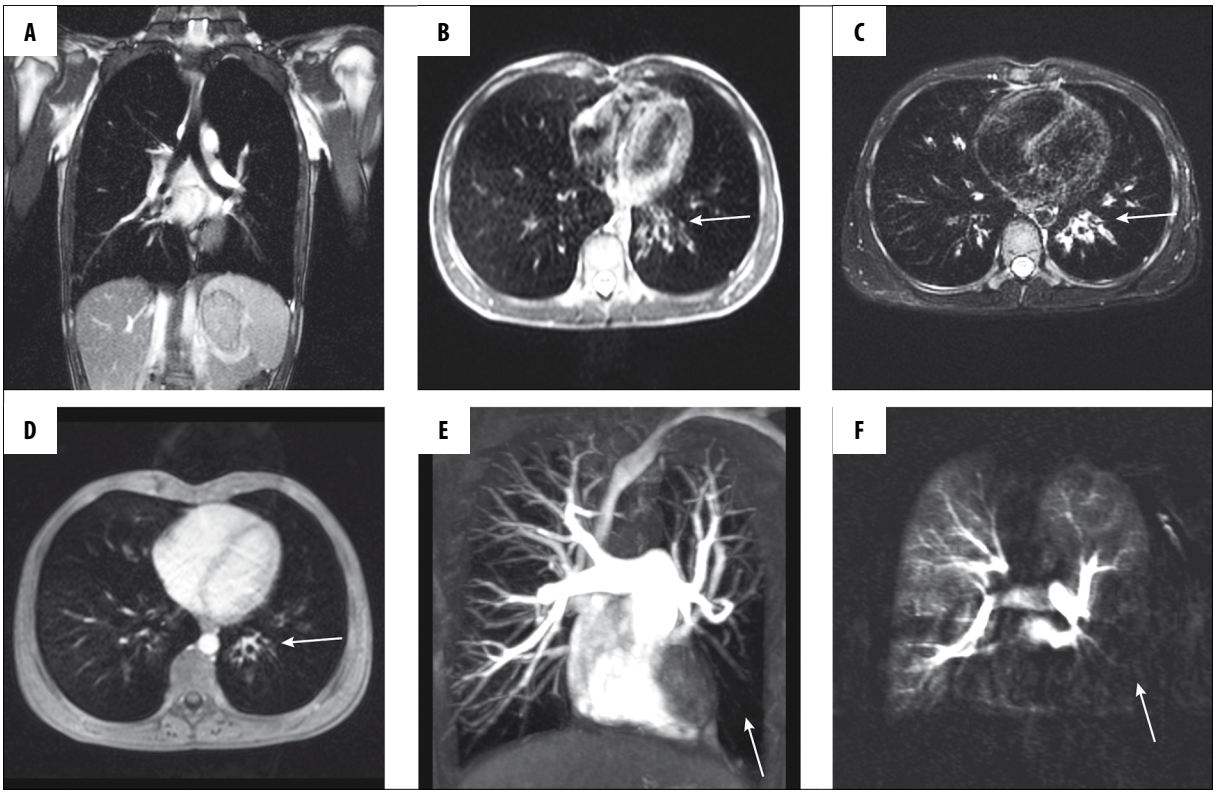

Figure 1. Images acquired in a 16 years old male patient with suspected Swyer James syndrome using different MR pulse sequences. The top row shows native coronal image obtained using bSSFP sequence (**A**) as well as transversal HASTE (**B**) and BLADE (**C**) acquisitions. In the bottom row 3D post-contrast transversal VIBE image (**D**) is shown. Of notice: bronchial wall thickening of the central left lower lobe bronchi (arrows) is visible in the transversal morphological images. The minimal intension projection (MIP) of a contrast enhanced FLASH 3D angiography shows rarefied pulmonary vessels in the left lower lobe (arrow) (**E**). Subtraction map of contrast enhanced MRI-perfusion measured with a TWIST sequence in the lung parenchymal phase visualizes a perfusion defect in the corresponding lobe (arrow).

and functional clinical chest protocols [25]. These robust pulse sequences use fast two- or three-dimensional techniques with short echo sampling to acquire the rapidly decaying signal. Application of multi-channel phased array coils allows for further acceleration of the data acquisition by using clinically available parallel imaging techniques such as generalized autocalibrating partially parallel acquisitions (GRAPPA) [26] or sensitivity encoding (SENSE) [27]. As a result the influence of motion can be partially suppressed. The simplest way in which the respiratory motion can be reduced is breath-holding. During a single inspiratory or expiratory breath-hold, images of the whole-lung volume can be acquired in about 20 s. However, for patients in poor condition breath-hold can be very demanding. A very popular method uses a navigator sequence to track the diaphragm movement during respiration. The use of navigator echoes allows the patient to continue breathing during the scan, and automatically triggers an imaging sequence to acquire data in an appropriate respiratory phase. During acquisition of the diagnostic data the navigator has to be turned off. Some of recently developed sequences have a build-in navigator for respiratory self-gating [28]. The artifacts associated with cardiac motion and blood pulsation can be minimized using either electrocardiogram monitoring or finger pulse sensor. The main drawback of gating techniques is remarkably prolonged acquisition time. As an alternative solution, other *k*-space sampling schemes characterized by intrinsic robustness against motion such as radial trajectory can be applied [29].

Current standard thorax imaging protocols comprise fast breath-hold sequences: fat-saturated T1-weighted three-dimensional gradient echo (3D GRE) known as volumetric interpolated breathhold acquisition (VIBE), T2-weighted half-Fourier acquisition single-shot turbo spin-echo (HASTE), as well as free-breathing sequences: balanced steady-state free precession (bSSFP), fat-saturated segmented radial turbo spin echo sequence with periodically rotated overlapping parallel lines with enhanced reconstruction (PROPELLER) aka BLADE [25] (Figure 1A–D). Contrast-enhanced protocol includes 3D GRE (volumetric interpolated breath-hold acquisition), high resolution angiography (Figure 1E), as well as perfusion measurement using dynamic contrast-enhanced MRI (Figure 1F), a technique described in detail in the further part of this article.

Hyperpolarized Gas Lung MRI

Not only hydrogen but also all nuclear magnetic resonance sensitive atoms can be used to generate MRI signal. For instance, inert noble gases possessing spin 1/2 such as ^{3}He and ^{129}Xe may serve as gaseous tracers that allow visualization of the ventilated airways and alveolar spaces. Since the density of these gases is too low to produce detectable signal, optical pumping must be applied to increase the amount of polarization per unit volume of gas. Two different techniques are used to polarize ^{3}He: spin exchange optical pumping (SEOP) [30,31] by the indirect transfer of angular moment from

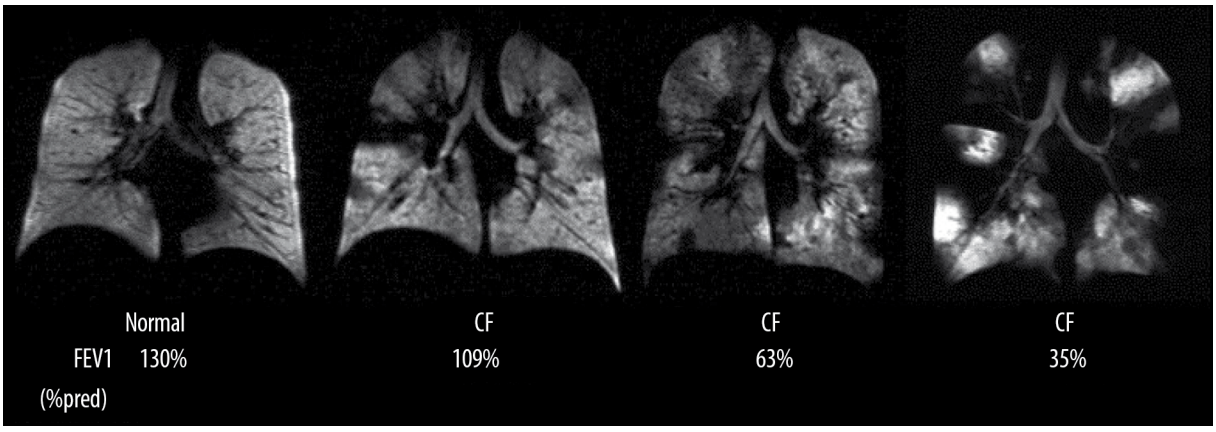

Figure 2. Coronal hyperpolarized ^{3}He MR ventilation images from a healthy subject and three patients with CF. Patients with CF have more ventilation defects than the healthy subject, and the number of defects increases with worsening FEV_1 (%predicted). From: Mentore K, et al., reprinted with permission from Ref. [51].

a laser source to the nucleus, or meta-stable spin exchange optical pumping (MEOP) [32] where a radio frequency discharge promotes a fraction of atoms into a metastable state and allows for direct transfer of the angular momentum from laser to the nucleus. With the use of this process, the so called hyperpolarization is obtained by increasing the difference between spin populations defined by the Boltzmann distribution by a factor of$\sim 10^5$. The magnetization decays with a characteristic relaxation time T_1 and is nonreversible. The gas can be stored for a period of a few days, which is sufficient to transport it to other imaging centers [33]. Hyperpolarized helium-3 is usually delivered to the subject for inhalation as a mixture with a larger volume of nitrogen. Due to the contact with paramagnetic oxygen in the lung the T_1 of the hyperpolarized ^{3}He is on order of 20–30 s, which is long enough to acquire the data from the whole lung volume. First images of the human lung using hyperpolarized ^{3}He were obtained in mid 1990s [34,35]. Since that time, the imaging methodology greatly improved and provides excellent quality to assess lung static and dynamic ventilation. Other applications in human studies include imaging of breathing dynamics [36,37], estimation of the apparent diffusion coefficient by exploiting the high diffusivity of helium [38,39], or measurements of oxygen partial pressure when ^{3}He is delivered for inhalation with a fraction of O_2 instead of N_2 [40,41].

During the last years, a significant clinical experience using ^{3}He MRI has been documented in the literature [42,43]. The technique has found application in studies of different pulmonary diseases including asthma [44–46], chronic obstructive lung disease (COPD) [47–49], cystic fibrosis [50–52], or bronchiolitis obliterans syndrome after lung transplantation [53–55]. Unlike in healthy subjects, where ventilation is homogenous throughout the lung and air spaces are filled simultaneously in all lung regions (Figure 2) in patients with airway diseases the ventilation distribution is patchy and none simultaneously. Despite the great potential of hyperpolarized ^{3}He MRI the main obstacle for its widespread clinical application is its limited supply, the sophisticated technical equipment for hyperpolarization and finally the very high price of the helium-3 isotope [56].

Another noble gas that can be used for MRI is ^{129}Xe. First experiments with hyperpolarized ^{129}Xe MRI were performed in the 1990s [57,58]. Due to the high natural abundance, it is much easier available for medical purposes in comparison to ^{3}He. Currently researchers are focused to translate the ^{3}He MRI methodology for xenon-129 based imaging. Despite the fact that it is more difficult to achieve high enough polarization using the SEOP method in ^{129}Xe, new efficient polarization systems have been constructed [59,60]. However, xenon-129 is characterized by a almost three times lower gyromagnetic ratio, therefore less MR signal can be detected. It exhibits relatively high solubility in blood and tissues as well as sensitivity to the environment, which results in a large chemical shift of about ~200 ppm relative to the gas-phase resonance frequency. This allows the acquisition of functional parameters characterizing the gas exchange but also gas uptake by imaging the dissolved-phase [61]. Recent work of Mugler et al. presents the possibility of gas- and dissolved-phase acquisition during a single scan [62]. By using xenon's diffusion property with xenon transfer contrast or chemical shift saturation recovery, various microstructure parameters including alveolar-volume ratio, blood-gas barrier thickness, and surface-to-volume ratio can be determined [63,64]. The major drawback of xenon-129 associated with solubility is its anesthetic property [65]. Therefore, the gas concentration must be kept on a safe level with continuous monitoring of the blood oxygenation level. The clinical experience with ^{129}Xe lung MRI is still limited to first case studies in groups of COPD and asthma subjects [66,67]. Thus, its safety and tolerability is a topic of current investigations.

Due to the recent advances in the polarization and imaging methodology, a quality comparable to ^{3}He MRI can be achieved by ^{129}Xe. Both hyperpolarized imaging techniques allow for the measurement of the whole-chest within a single breathhold using 5 to 10 mm thick sections with up to 1 mm in-plane resolution. For implementations on a 1.5T and 3T field strength, multi-slice 2D or 3D acquisitions with fast low angle shot (FLASH) or balanced steady-state free precession (bSSFP) sequences are generally used [68].

In view of a the requirement for sophisticated equipment and relatively high production costs of hyperpolarized tracers these imaging techniques are so far only available at a limited number of research centers and not validated yet for clinical use.

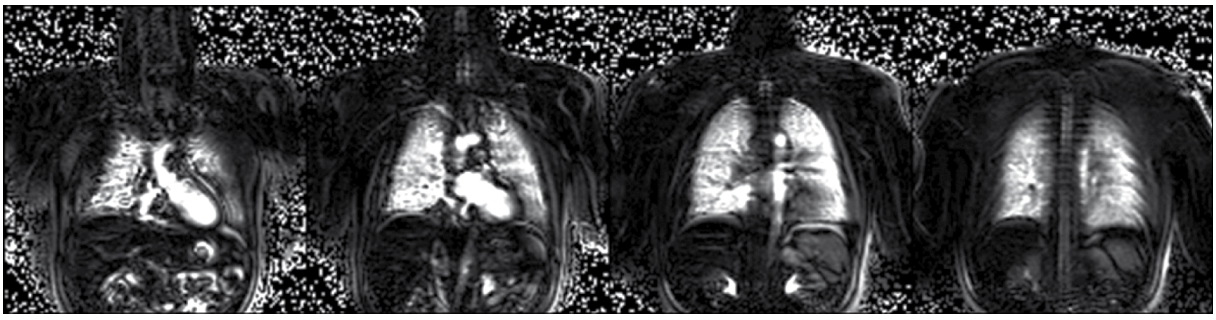

Figure 3. Oxygen-enhanced subtraction MR images in four coronal slices of a healthy volunteer acquired using an ECG-triggered HASTE pulse sequence in breathhold. Images courtesy of F. Molinari (Department of Bioimaging and Radiological Sciences, Catholic University of Rome, Italy).

Oxygen Enhanced MRI

Application of molecular oxygen as a contrast medium for conventional ^{1}H MRI of the lung was first suggested by Edelman et al. [69]. Inhalation of oxygen-enriched gas increases the partial oxygen pressure in the pulmonary alveoli and the oxygen diffusion from alveoli into the blood capillaries [70]. Paramagnetic properties of dissolved molecular oxygen and deoxyhemoglobin cause a T_1-shortening effect, which is proportional to the oxygen concentration in the inhaled gas [71]. The reduced relaxation time enhances the signal intensity in T_1-weighted imaging, and allows for determination of regional oxygen transfer influenced by pulmonary ventilation, perfusion and diffusion. Thus, regions with impeded lung function can be visualized. Since the application of oxygen-enhanced (OE) MRI is easy to implement and inexpensive, different studies have been conducted for evaluation of this technique.

The simplest way in which the imaging can be performed is by acquisition of two separate data sets. The first set of images is measured when breathing room air. Subsequently, oxygen at a flow rate of 15–25 L/min is administered through a mask for several minutes to achieve a steady-state concentration in the lung, which continues during the acquisition of the second data set. A subtraction image or a map showing relative difference of the signal enhancement can be calculated. Figure 3 shows an example of oxygen-enhanced images obtain in a healthy volunteer. The image acquisition of both sets is performed in breath-hold, as a consequence misregistration artifacts especially in the diaphragmatic regions may occur. To minimize this effect triggering or image registration techniques must be applied [72,73]. Also the influence of the blood flow and cardiac pulsation on the signal intensity should not be neglected. The second imaging method is based on the data acquisition during the wash-in process. Analysis of the signal slope for different concentration of oxygen provides additional information allowing for calculation of so-called oxygen transfer function, which can correlate with a pulmonary pathology [74,75].

Furthermore, using OE MRI it is also possible to measure regional changes of T_2* [76]. This approach, however, is very difficult since the measured change in the extremely short relaxation time is minimal. To summarize, OE MRI is a safe and easily implementable method to assess the lung function. For a routine clinical use, the major disadvantage of this technique is very long examination time. Thus, the majority of studies were limited to acquire only single or several 2D slices. Secondly, OE MRI does not provide a direct measure of ventilation; it is influenced by pulmonary perfusion and oxygen diffusion.

Perfusion Dynamic Contrast-Enhanced MRI

Evaluation of lung perfusion is of particular interest for diagnosis of different pulmonary diseases. Pulmonary perfusion is strongly influenced by regional ventilation. Both parameters are kept in balance, which is required for efficient gas exchange. Hypoxic vasoconstriction plays here a significant role to prevent localized ventilation/perfusion mismatching by reduction of the blood flow to the unventilated lung regions [77]. In other cases the perfusion can be reduced without impairment of ventilation as a result of pulmonary embolism.

Several MRI techniques have been described to image lung perfusion. The well-established and increasingly popular method, which has shown a particular usefulness for diagnosis and differentiation of different lung pathologies, is known as dynamic contrast-enhanced (DCE) imaging [78]. The basic principle of DCE MRI is time-resolved data acquisition following an intravenous bolus injection of a paramagnetic contrast agent such as gadolinium diethylenetraminepentaacetic acid (Gd-DTPA). The injected contrast agent circulates through the body and diffuses into the extravascular extracellular space. Increase of the local contrast agent concentration results in a reduction of the longitudinal relaxation time T_1 and signal enhancement in a voxel. Application of 3D T1-weighted sequences enables tracking the signal enhancement in the whole lungs as the contrast passes through the pulmonary circulation. The acquired data can be analyzed by visual assessment, calculation of descriptive parameters, or quantitative parameters using different tracer kinetic theories [79]. For the visual assessment of DCE MRI often a simple subtraction of the data obtained during the peak signal enhancement and before contrast agent administration is used. Regions with reduced parenchymal perfusion are identified as areas of low contrast enhancement (Figures 1F and 6A). This method, however, neglects the majority of information contained in the temporal component of the dynamic acquisition. Another simple and practical analysis of DCE images is based on estimation of additional parameters describing the signal curve such as time to peak enhancement, bolus arrival time, and maximum enhancement [80] (Figure 4).

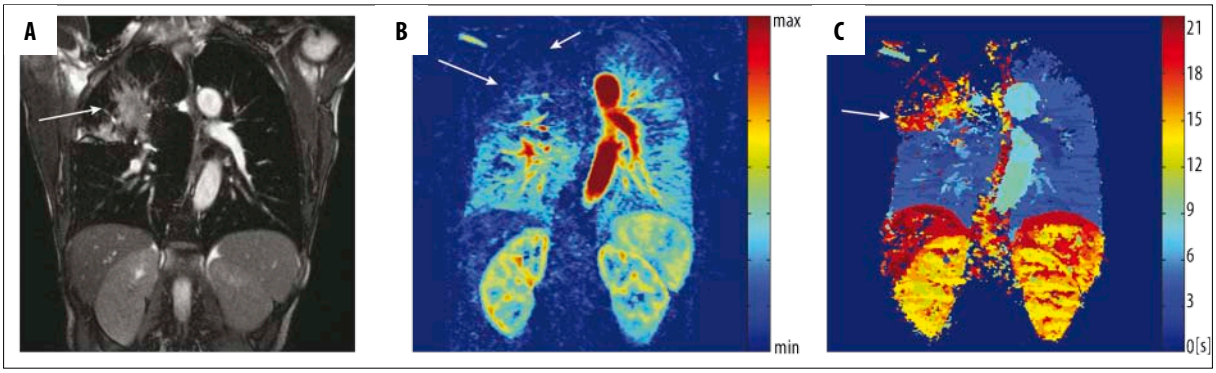

Figure 4. Morphological coronal bSSFP image (**A**) acquired in a 55 year old patient with bronchial carcinoma stage III (arrow) in the right upper lobe. DCE MRI was used to calculate the maps of the maximum contrast enhancement (**B**) and time to peak (**C**). The signal amplitude in parenchymal tissue in the upper lobe of the right lung is remarkably reduced on the maximum contrast enhanced map (arrows). Time to peak map shows delay in contrast agent inflow to the cancerous tissue (arrow).

By combining this approach with statistical analysis of the semi-quantitative parameters and automatic lung segmentation is possible to estimate percentage of perfusion defects per lung region, which is similar to the information usually obtained from SPECT data [81]. A more complex analysis of pulmonary perfusion using the indicator dilution theory allows for quantitative estimation of pulmonary blood volume, pulmonary blood flow and mean transit time [78,82–84]. The calculations are based on pixel-wise numerical deconvolution of the contrast concentration curve and arterial input function obtained from the time-resolved data set. In order to obtain correct physiological values it is important to assure a linear relationship between the local contrast agent concentration and MR signal intensity [85], which is given only at very low concentrations of applied contrast media. Furthermore, the results can be strongly influenced by respiratory motion and high noise level.

Different studies have been performed for the evaluation of the diagnostic value of DCE MRI in patients with pulmonary embolism [86,87], COPD [88], cystic fibrosis [89,90], pulmonary hypertension [91,92], as well as in oncologic field for detection of bronchial carcinoma, or evaluation of postoperative lung function [93]. The technique was also validated against standard clinical tools including scintigraphy, SPECT and CT [93,94] as well as tested for its reproducibility [95]. Up to now it is the best validated MR perfusion imaging method with well documented clinical impact in the early diagnosis of cystic fibrosis and the assessment of therapy response [96,97].

Current imaging protocols for DCE MRI include 3D fast low angle shot (FLASH), time-resolved echo-shared angiographic technique (TREAT), time-resolved imaging of contrast kinetics (TRICKS), or time resolved angiography with interleaved stochastic trajectories (TWIST) imaging sequences [98–100]. By application of parallel imaging and view sharing techniques these sequences offer a very good spatial and temporal resolution of about 1.5×1.5 mm^2 with 5 mm section thickness and the acquisition rate of 2 volumes per second.

Despite the fact that gadolinium based contrast agents are generally well tolerated by the vast majority of patients there is a limit in the total amount of contrast material, which can be introduced intravenously to the patient in a given period of time, limiting the number of possible acquisitions. There are known risks associated with the use gadolinium based contrast agent, which include acute allergic reactions and a possibility of development of nephrogenic systemic fibrosis in patients with severely impaired renal function [101,102]. Furthermore, administration of contrast agents should be also carefully considered in neonates or infants up to one year of age because the effect of Gd-DTPA on the still developing kidney in these age groups is not well understood.

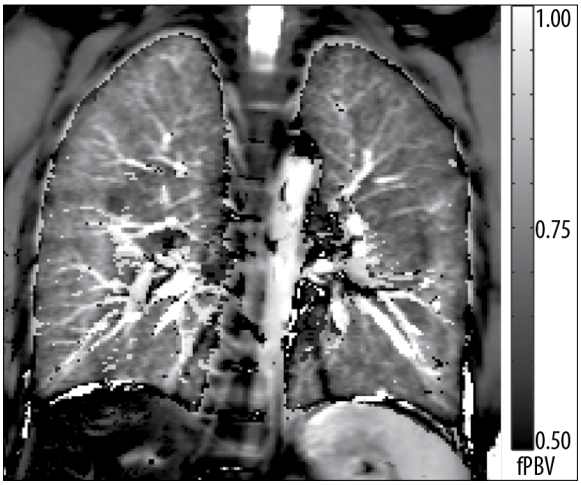

Figure 5. The map shows a homogenous distribution of the fractional pulmonary blood volume (fPBV) within the lung parenchyma of a healthy volunteer. Small vessels as well as the aorta are distinctly displayed. The hilar region shows scattered noticeably small fPBV-values. This can be ascribed to residual pulsation artifacts near major blood vessels. Remaining diaphragmatic movement explains artifacts at the thoracic-abdominal interface.

Non-Contrast-Enhanced Imaging Techniques

So far, all presented techniques in this article require the administration of gaseous tracers or injection of intravenous contrast media for assessment of pulmonary ventilation and perfusion. In the last years, alternative non-contrast-enhanced imaging methods have received much attention. One of them is pulmonary perfusion arterial

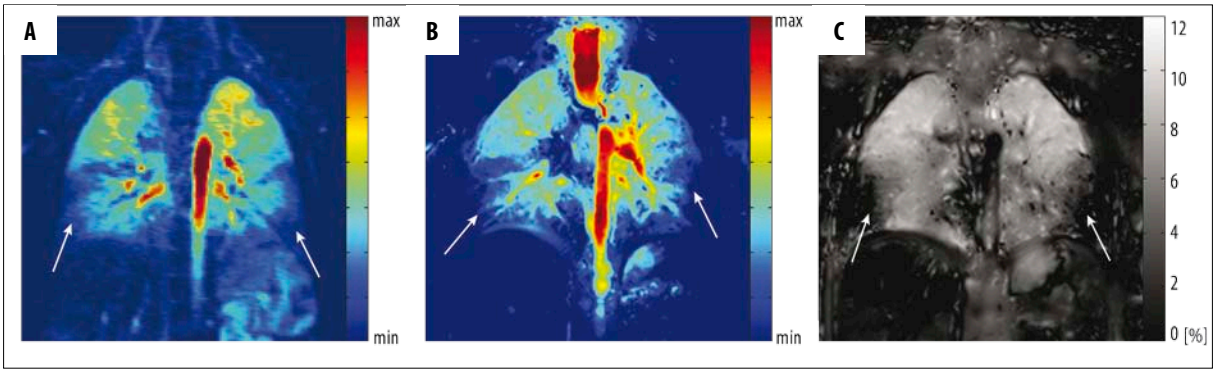

Figure 6. Coronal images acquired in a 5 year old male cystic fibrosis patient. DCE MRI (**A**) shows perfusion defects in the lower lobes of the right and left lung. Identical pattern of regions with reduced perfusion can be recognized on contrast agent free perfusion-weighted FD MRI (**B**). Furthermore, the ventilation-weighted FD MRI (**C**) shows decreased percental change of the pulmonary tissue density in underperfused lung areas, visualizing areas of reduced ventilation (**C**) and hypoxic vasoconstriction (**B**).

spin labeling (ASL) MRI [103,104]. This technique is well-known from cerebral perfusion measurements. It uses magnetically-tagged water protons in arterial blood as a contrast bolus to measure blood delivery to the lung tissue. Blood is tagged by application of radio frequency pulses to invert the magnetization. ASL is based on acquisition of so-called control and tag images at the same anatomical location using different schemes of magnetization inversion [105]. A perfusion map is produced by subtraction of these images and application of a quantitative model for estimation of the pulmonary blood flow [106]. Nevertheless, the implementation of this non-invasive technique for thoracic imaging is difficult due to respiratory motion and signal change induced by pulmonary blood flow. Image acquisition is usually performed using an ECG-triggered 2D HASTE sequence at 1.5 T. To measure the small signal difference in the lung parenchyma a certain number of averages is required to obtain reasonable signal-to-noise ratio, which can significantly prolong the examination time.

Recently, a two-compartment inversion recovery (TCIR) technique was proposed for quantitative regional estimation of the fractional pulmonary blood volume (fPBV) without the application of contrast media [107]. The method assumes that total signal measured in the lung parenchyma arises from intravascular and extravascular protons. By performing a series of inversion recovery experiments it is possible to separate both signal components characterized by different longitudinal relaxation times, resulting in a map of the fPBV. Similarly to ASL this technique is based on ECG-triggered 2D HASTE sequence and is able to produce high resolution maps of the fPBV. Figure 5 shows an example of a fPBV map measured in a healthy volunteer.

One of the latest developments in the field of functional lung ^{1}H MRI is known as Fourier decomposition (FD) method [108,109]. This non-invasive technique provides both ventilation-weighted (Vw) and perfusion-weighted (Qw) information from a single acquisition series and requires no administration of contrast media, as well as no further patient compliance such as repeated, or prolonged breath hold. The imaging is performed using a 2D multislice time-resolved bSSFP pulse sequence in free breathing. In order to increase the signal intensity from the lung parenchyma an asymmetric sampling of very short echo time combined with parallel imaging is applied. Each image within the acquired data set is registered to a chosen reference image for correction of respiratory motion [110]. Two physiological processes, respiration and cardiac cycle influence the signal intensity in the lung by the deformation of the pulmonary tissue and blood dependent signal dephasing, respectively [111,112]. Signal intensity values are measured during expiration and diastolic heart phase are higher than the values in inspiration and systolic phase. Pixel-wise Fourier analysis can be used to separate these periodic signal intensity variations at the respiratory and cardiac frequencies. Amplitude of the regional signal intensity modulation is used to generate Vw and Qw images. The technique was recently qualitatively validated with the clinical gold-standard ventilation/perfusion SPECT measurements in a large-scale animal model [113]. Nevertheless, the quantitative signal analysis in FD MRI is still a subject to further investigation. Initial studies in healthy volunteers and cystic fibrosis patients have shown the feasibility of this technique to detect functional lung changes [114]. Figure 6 shows Vw and Qw images obtained in a cystic fibrosis patient in comparison to DCE MRI from a corresponding slice location. The technique is implementable on routine clinical equipment and requires 10–15 minutes examination time to cover the whole lung volume.

Conclusions

Along with the progress in the MR technology the functional lung imaging undergoes a dynamic evolution. Development of new approaches for the assessment of the lung function is motivated by scientific questions regarding the human lung physiology and pathophygiology of pulmonary diseases, as well as by the need for fast and robust clinically applicable imaging techniques. Functional lung parameters obtained using MRI provide often complementary information to standard imaging modalities. The strength of MRI is especially notable in the field of dynamic imaging allowing for tracking fast physiological changes in regional ventilation and perfusion. Due to the increasing availability, MRI can be a promising ionizing-free alternative to techniques like computed tomography or nuclear medicine techniques for the evaluation of lung function.

References:

1. Altalag A, Road J, Wilcox P: Pulmonary Function Tests in Clinical Practice. Springer-Verlag London Limited, London, UK, 2009, 1–37
2. de Jong PA, Nakano Y, Lequin MH et al: Progressive damage on high resolution computed tomography despite stable lung function in cystic fibrosis. Eur Respir J, 2004; 23(1): 93–97
3. Wagner PD: The multiple inert gas elimination technique (MIGET). Intensive Care Med, 2008; 34: 994–1001
4. Anderson JC, Hlastala MP: Impact of airway gas exchange on the multiple inert gas elimination technique: theory. Ann Biomed Eng, 2010; 38(3): 1017–30
5. Gustafsson PM, Aurora P, Lindblad A: Evaluation of ventilation maldistribution as an early indicator of lung disease in children with cystic fibrosis. Eur Respir J, 2003; 22(6): 972–79
6. Fuchs SI, Buess C, Lum S et al: Multiple breath washout with a sidestream ultrasonic flow sensor and mass spectrometry: a comparative study. Pediatr Pulmonol, 2006; 41(12): 1218–25
7. Thia L, Hoo AF, Nguyen TD et al: Improvement in lung function during the 1st year of life in infants diagnosed with CF through newborn screening (NBS); Abstract 4656, ERS Congress 2011, Amsterdam
8. Patz EF, Coleman RE: Nuclear medicine techniques. In: Mason RJ, Murray J, Broaddus VC, Nadel J (eds.): Textbook of Respiratory Medicine. Saunders Elsevier, Philadelphia, PA, USA, 2005; 594–99
9. Roach PJ, Bailey DL, Harris BE: Enhancing lung scintigraphy with single-photon emission computed tomography. Semin Nucl Med. 2008, 38(6): 441–99
10. Vidal Melo MF, Layfield D, Harris RS et al: Quantification of regional ventilation-perfusion ratios with PET. J Nucl Med, 2003; 44: 1982–91
11. Thieme SF, Hoegl S, Nikolaou K et al: Pulmonary ventilation and perfusion imaging with dual-energy CT. Eur Radiol, 2010; 20(12): 2882–89
12. Chae EJ, Seo JB, Goo HW et al: Xenon ventilation CT with a dual-energy technique of dual-source CT: initial experience. Radiology, 2008; 248(2): 615–24
13. Donadieu J, Roudier C, Saguintaah M et al: Estimation of the radiation dose from thoracic CT scans in a cystic fibrosis population. Chest, 2007; 132(4): 1233–38
14. Revel MP, Cohen S, Sanchez O et al: Pulmonary embolism during pregnancy: diagnosis with lung scintigraphy or CT angiography? Radiology, 2011;258(2): 590–98
15. Plathow C, Ley S, Fink C et al: Evaluation of lung volumetry using dynamic three-dimensional magnetic resonance imaging. Invest Radiol, 2004; 40(3): 173–79
16. Tetzlaff R, Schwarz T, Kauczor HU et al: Function Measurement of Single Lungs by Lung Area Segmentation on 2D Dynamic MRI. Acad Radiol, 2010; 17(4): 496–503
17. Swift AJ, Woodhouse N, Fichele S et al: Rapid lung volumetry using ultrafast dynamic magnetic resonance imaging during forced vital capacity maneuver: correlation with spirometry. Invest Radiol, 2007, 42(1): 37–41
18. Cutillo AG (eds.): Application of Magnetic Resonance to the Study of Lung, 1996, Futura Publishing Company, Inc., Armonk, NY, USA
19. Landwehr P, Schulte O, Lackner K: MR imaging of the chest: mediastinum and chest wall. Eur Radiol 1999; 9(9): 1737–44
20. Pedersen MR, Fisher MT, van Beek EJ: MR imaging of the pulmonary vasculature – an update. Eur Radiol, 2006; 16(6): 1374–86
21. Long FR, Williams RS, Castile RG: Inspiratory and expiratory CT lung density in infants and young children. Pediatr Radiol, 2005, 35: 677–83
22. Hatabu H, Alsop DC, Listerud J et al: T2* and proton density measurement of normal human lung parenchyma using submillisecond echo time gradient echo magnetic resonance imaging. Eur J Radiol, 1999; 29: 245–52
23. Stadler A, Jakob PM, Griswold M et al: T1 mapping of the entire lung parenchyma: Influence of the respiratory phase in healthy individuals. J Magn Reson Imaging, 2005; 21: 759–64
24. Fink C, Puderbach M, Biederer J et al: Lung MRI at 1.5 and 3 Tesla: observer preference study and lesion contrast using five different pulse sequences. Invest Radiol, 2007; 42(6): 377–83
25. Puderbach M, Hintze C, Ley S et al: MR imaging of the chest: a practical approach at 1.5T. Eur J Radiol, 2007;64(3): 345–55
26. Griswold MA, Jakob PM, Heidemann RM et al: Generalized autocalibrating partially parallel acquisitions (GRAPPA). Magn Reson Med, 2002; 47(6): 1202–10
27. Pruessmann KP, Weiger M, Scheidegger MB et al: SENSE: sensitivity encoding for fast MRI. Magn Reson Med, 1999; 42(5): 952–62
28. Weick S, Oechsner M, Blaimer M et al: Self-gated 3D FLASH imaging of the human lung under free breathing using DC signals. Proceedings of the 17th Annual Meeting of ISMRM, Honolulu, Hawaii, USA, 2009; 2009
29. Block KT, Uecker M, Frahm J: Undersampled radial MRI with multiple coils. Iterative image reconstruction using a total variation constraint. Magn Reson Med, 2007; 57(6): 1086–98
30. Bouchiat M, Carver T, Varnum C: Nuclear polarization in 3He gas induced by optical pumping and dipolar exchange. Phys Rev Lett, 1960; 5: 373–75
31. Appelt S, Ben-Amar Baranga A, Rickson J et al: Theory of spin-exchange optical pumping of ^{3}He and ^{129}Xe. Phys Rev A, 1998; 58: 1412–39
32. Colegrove F: Polarization of He-3 gas by optical pumping. Phys Rev, 1963; 132: 2561
33. Wild JM, Schmiedeskamp J, Paley MN et al: MR imaging of the lungs with hyperpolarized helium-3 gas transported by air. Phys Med Biol, 2002; 47: 185–90
34. Middleton H, Black RD, Saam B: MR imaging with hyperpolarized 3He gas. Magn Reson Med, 1995; 33: 271–75
35. Ebert M, Grossmann T, Heil W et al: Nuclear magnetic resonance imaging with hyperpolarised helium-3. Lancet, 1996; 347: 1297–99
36. Wild JM, Paley MN, Kasuboski L et al: Dynamic radial projection MRI of inhaled hyperpolarized 3He gas. Magn Reson Med, 2003; 49: 991–97
37. Holmes JH, O'Halloran RL, Brodsky EK: Three-dimensional imaging of ventilation dynamics in asthmatics using multiecho projection acquisition with constrained reconstruction. Magn Reson Med. 2009; 62(6): 1543–56
38. Habib D, Grebenkov D, Guillot G: Gas diffusion in a pulmonary acinus model: experiments with hyperpolarized helium-3. Magn Reson Imaging, 2008; 26(8): 1101–13
39. Mugler JP III, Wang C, Miller GW et al: Helium-3 diffusion MR imaging of the human lung over multiple time scales. Acad Radiol, 2008; 15(6): 693–701
40. Deninger AJ, Eberle B, Ebert M et al: (3)he-MRI-based measurements of intrapulmonary p(O2) and its time course during apnea in healthy volunteers: first results, reproducibility, and technical limitations. NMR Biomed, 2000; 13(4): 194–201
41. Miller GW, Mugler JP III, Altes TA et al: A short-breath-hold technique for lung pO_2 mapping with ^{3}He MRI. Magn Reson Med, 2010; 63(1): 127–36
42. Altes TA, Salerno M: Hyperpolarized gas MR imaging of the lung. J Thorac Imaging. 2004; 19(4): 250–58
43. Fain S, Schiebler ML, McCormack DG et al: Imaging of lung function using hyperpolarized helium-3 magnetic resonance imaging: Review of current and emerging translational methods and applications. J Magn Reson Imaging, 2010; 32(6): 1398–408
44. Altes TA, Powers PL, Knight-Scott J et al: Hyperpolarized 3He MR lung ventilation imaging in asthmatics: preliminary findings. J Magn Reson Imaging, 2001; 13(3): 378–84
45. de Lange EE, Altes TA, Patrie JT et al: Evaluation of asthma with hyperpolarized helium-3 MRI: correlation with clinical severity and spirometry. Chest, 2006; 130(4): 1055–62
46. Fain SB, Gonzalez-Fernandez G, Peterson ET et al: Evaluation of structure-function relationships in asthma using multidetector CT and hyperpolarized He-3 MRI. Acad Radiol, 2008; 15(6): 753–62
47. Saam B, Yablonskiy D, Kodibagkar V et al: MR imaging of diffusion of 3He gas in healthy and diseased lungs. Magn Reson Med, 2000; 44: 174–79
48. van Beek EJ, Dahmen AM, Stavngaard T et al: Hyperpolarised ^{3}He MRI versus HRCT in COPD and normal volunteers: PHIL trial. Eur Respir J, 2009; 34(6): 1311–21

49. Kirby M, Mathew L, Wheatley A et al: Chronic obstructive pulmonary disease: longitudinal hyperpolarized (3)He MR imaging. Radiology, 2010; 256(1): 280–89
50. Donnelly LF, MacFall JR, McAdams HP et al: Cystic fibrosis: combined hyperpolarized 3He-enhanced and conventional proton MR imaging in the lung - preliminary observations. Radiology, 1999; 212(3): 885–89
51. Mentore K, Froh DK, de Lange EE et al: Hyperpolarized HHe 3 MRI of the lung in cystic fibrosis: assessment at baseline and after bronchodilator and airway clearance treatment. Acad Radiol, 2005; 12(11): 1423–29
52. Bannier E, Cieslar K, Mosbah K et al: Hyperpolarized ^{3}He MR for sensitive imaging of ventilation function and treatment efficiency in young cystic fibrosis patients with normal lung function. Radiology, 2010; 255(1): 225–32
53. McAdams HP, Palmer SM, Donnelly LF et al: Hyperpolarized ^{3}He-enhanced MR imaging of lung transplant recipients: preliminary results. AJR Am J Roentgenol, 1999; 173(4): 955–59
54. Lipson DA, Roberts DA, Hansen-Flaschen J et al: Pulmonary ventilation and perfusion scanning using hyperpolarized helium-3 MRI and arterial spin tagging in healthy normal subjects and in pulmonary embolism and orthotopic lung transplant patients. Magn Reson Med, 2002; 47(6): 1073–76
55. Gast KK, Biedermann A, Herweling A et al: Oxygen-sensitive ^{3}He-MRI in bronchiolitis obliterans after lung transplantation. Eur Radiol, 2008; 18(3): 530–37
56. Shea DA, Morgan D: The Helium-3 Shortage: Supply, Demand, and Options for Congress. [Federation of American Scientists Web site]. *http://www.fas.org/sgp/crs/misc/R41419.pdf* (accessed 08.07.2011)
57. Albert MS, Cates GD, Driehuys B et al: Biological magnetic resonance imaging using laser-polarized 129Xe. Nature, 1994; 370: 199–201
58. Mugler JP III, Driehuys B, Brookeman JR et al: MR imaging and spectroscopy using hyperpolarized ^{129}Xe gas: preliminary human results. Magn Reson Med, 1997; 37(6): 809–15
59. Ruset IC, Ketel S, Hersman FW: Optical pumping system design for large production of hyperpolarized Xe-129. Phys Rev Lett, 2006; 96
60. Hersman FW, Ruset IC, Ketel S et al: Large production system for hyperpolarized ^{129}Xe for human lung imaging studies. Acad Radiol 2008; 15: 683–92
61. Wagshul ME, Button TM, Li HF et al: *In vivo* MR imaging and spectroscopy using hyperpolarized ^{129}Xe. Magn Reson Med, 1996; 36(2): 183–91
62. Mugler JP III, Altes TA, Ruset IC et al: Simultaneous magnetic resonance imaging of ventilation distribution and gas uptake in the human lung using hyperpolarized xenon-129. Proc Natl Acad Sci USA, 2010; 107(50): 21707–12
63. Ruppert K, Brookeman JR, Hagspiel KD, Mugler JP III: Probing lung physiology with xenon polarization transfer contrast (XTC). Magn Reson Med, 2000; 44(3): 349–57
64. Patz S, Muradian I, Hrovat MI et al: Human pulmonary imaging and spectroscopy with hyperpolarized ^{129}Xe at 0.2T. Acad Radiol, 2008; 15(6): 713–27
65. Latchaw RE, Yonas H, Pentheny SL, Gur D: Adverse reactions to xenon-enhanced CT cerebral blood flow determination. Radiology, 1987; 163: 251–54
66. Dregely I, Mugler JP III, Ruset IC et al: Hyperpolarized Xenon-129 gas-exchange imaging of lung microstructure: first case studies in subjects with obstructive lung disease. J Magn Reson Imaging, 2011; 33(5): 1052–62
67. Kaushik SS, Cleveland ZI, Cofer GP et al: Diffusion-weighted hyperpolarized 129Xe MRI in healthy volunteers and subjects with chronic obstructive pulmonary disease. Magn Reson Med, 2011; 65(4): 1154–65
68. Wild JM, Teh K, Woodhouse N et al: Steady-state free precession with hyperpolarized 3He: experiments and theory. J Magn Reson, 2006; 183(1): 13–24
69. Edelman RR, Hatabu H, Tadamura E et al: Noninvasive assessment of regional ventilation in the human lung using oxygen-enhanced magnetic resonance imaging. Nat Med, 1996; 2: 1236–39
70. Brooks RA, Di Chiro G: Magnetic resonance imaging of stationary blood: a review. Med Phys, 1987; 14: 903–13
71. Ohno Y, Chen Q, Hatabu H: Oxygen-enhanced magnetic resonance ventilation imaging of lung. Eur J Radiol, 2001; 37: 164–71
72. Molinari F, Eichinger M, Risse F et al: Navigator-triggered oxygen-enhanced MRI with simultaneous cardiac and respiratory synchronization for the assessment of interstitial lung disease. J Magn Reson Imaging, 2007; 26(6): 1523–29
73. Molinari F, Bauman G, Paolantonio G et al: Improvement of multislice oxygen-enhanced MRI of the lung by fully automatic non-rigid image registration. Eur J Radiol, 2011 [Epub ahead of print]
74. Jakob PM, Wang T, Schultz G et al: Assessment of human pulmonary function using oxygen-enhanced T(1) imaging in patients with cystic fibrosis. Magn Reson Med, 2004; 51(5): 1009–16
75. Stadler A, Stiebellehner L, Jakob PM et al: Quantitative and o(2) enhanced MRI of the pathologic lung: findings in emphysema, fibrosis, and cystic fibrosis. Int J Biomed Imaging, 2007; 2007: 23624
76. Pracht ED, Arnold JF, Wang T, Jakob PM: Oxygen-enhanced proton imaging of the human lung using T2. Magn Reson Med, 2005; 53: 1193–96
77. Euler US, Liljestrand G: Observations on the Pulmonary Arterial Blood Pressure in the Cat. Acta Phys Scandinav, 1947; 12: 301–20
78. Hatabu H, Gaa J, Kim D et al: Pulmonary perfusion: qualitative assessment with dynamic contrast-enhanced MRI using ultra-short TE and inversion recovery turbo FLASH. Magn Reson Med 1996; 36(4): 503–8
79. Rosen BR, Belliveau JW, Vevea JM, Brady TJ: Perfusion imaging with NMR contrast agents. Magn Reson Med, 1990; 14(2): 249–65
80. Risse F, Eichinger M, Kauczor HU et al: Improved visualization of delayed perfusion in lung MRI. Eur J Radiol, 2011; 77(1): 105–10
81. Heimann T, Eichinger M, Bauman G et al: Automated Scoring of Regional Lung Perfusion in Children from contrast enhanced 3D MRI. Proceedings of SPIE, San Diego, CA, USA, 2012; 8315–29
82. Levin DL, Chen Q, Zhang M et al: Evaluation of regional pulmonary perfusion using ultrafast magnetic resonance imaging. Magn Reson Med, 2001; 46(1): 166–71
83. Fink C, Risse F, Buhmann R et al: Quantitative analysis of pulmonary perfusion using time-resolved parallel 3D MRI – initial results. Rofo, 2004; 176(2): 170–74
84. Nikolaou K, Schoenberg SO, Brix G et al: Quantification of pulmonary blood flowand volume in healthy volunteers by dynamic contrast-enhanced magnetic resonance imaging using a parallel imaging technique. Invest Radiol, 2004; 39(9): 537–45
85. Puderbach M, Risse F, Biederer J et al: *In vivo* Gd-DTPA concentration for MR lung perfusion measurements: assessment with computed tomography in a porcine model. Eur Radiol, 2008; 18(10): 2102–7
86. Amundsen T, Torheim G, Kvistad KA et al: Perfusion abnormalities in pulmonary embolism studied with perfusion MRI and ventilation-perfusion scintigraphy: an intra-modality and inter-modality agreement study. J Magn Reson Imaging, 2002; 15(4): 386–94
87. Kluge A, Gerriets T, Lange U, Bachman G: MRI for short-term follow-up of acute pulmonary embolism. Assessment of thrombus appearance and pulmonary perfusion: a feasibility study. Eur Radiol, 2005; 15(9): 1969–77
88. Ley-Zaporozhan J, Ley S, Eberhardt R et al: Assessment of the relationship between lung parenchymal destruction and impaired pulmonary perfusion on a lobar level in patients with emphysema. Eur J Radiol, 2007; 63(1): 76–83
89. Eichinger M, Puderbach M, Fink C et al: Contrast-enhanced 3D MRI of lung perfusion in children with cystic fibrosis – initial results. Eur Radiol, 2006; 16(10): 2147–52
90. Eichinger M, Optazaite DE, Kopp-Schneider A et al: Morphologic and functional scoring of cystic fibrosis lung disease using MRI. Eur J Radiol, 2011 [Epub ahead of print]
91. Nikolaou K, Schoenberg SO, Attenberger U et al: Pulmonary arterial hypertension: diagnosis with fast perfusion MR imaging and high-spatial-resolution MR angiography – preliminary experience. Radiology, 2005; 236(2): 694–703
92. Ley S, Mereles D, Risse F et al: Quantitative 3D pulmonary MR-perfusion in patients with pulmonary arterial hypertension: correlation with invasive pressure measurements. Eur J Radiol, 2007; 61(2): 251–55
93. Molinari F, Fink C, Risse F et al: Assessment of differential pulmonary blood flow using perfusion magnetic resonance imaging: comparison with radionuclide perfusion scintigraphy. Invest Radiol, 2006; 41(8): 624–30

94. Kluge A, Gerriets T, Stolz E et al: Pulmonary perfusion in acute pulmonary embolism: agreement of MRI and SPECT for lobar, segmental and subsegmental perfusion defects. Acta Radiol, 2006; 47(9): 933–40
95. Ley-Zaporozhan J, Molinari F, Risse F et al: Repeatability and reproducibility of quantitative whole-lung perfusion magnetic resonance imaging. J Thorac Imaging. 2011; 26(3): 230–39
96. Puderbach M, Eichinger M, Haeselbarth J et al: MRI for early Diagnosis of Lung Changes in Children with Cystic Fibrosis. Am J Resp Crit Care Med, 2008; 177: 224
97. Eichinger M, Haeselbarth J, Niemann A et al: Magnetic-resonance-imaging (MRI) for assessment of regional therapy response in Patients with Cystic Fibrosis (CF). Eur Respir J, 2009; 53(Suppl.): 34
98. Korosec FR, Frayne R, Grist TM, Mistretta CA: Time-resolved contrast-enhanced 3D MR angiography. Magn Reson Med, 1996; 36(3): 345–51
99. Fink C, Ley S, Kroeker R et al: Time-resolved contrast-enhanced three-dimensional magnetic resonance angiography of the chest: combination of parallel imaging with view sharing (TREAT). Invest Radiol, 2005; 40(1): 40–48
100. Lim RP, Shapiro M, Wang EY et al: 3D time-resolved MR angiography (MRA) of the carotid arteries with time-resolved imaging with stochastic trajectories: comparison with 3D contrast-enhanced Bolus-Chase MRA and 3D time-of-flight MRA. AJNR Am J Neuroradiol, 2008; 29(10): 1847–54
101. Zou Z, Zhang HL, Roditi GH et al: Nephrogenic systemic fibrosis review of 370 biopsy-confirmed cases. JACC Cardiovasc Imaging. 2011; 4(11): 1206–16
102. Gauden AJ, Phal PM, Drummond KJ: MRI safety: nephrogenic systemic fibrosis and other risks. J Clin Neurosci, 2010; 17(9): 1097–104
103. Mai VM, Berr SS: MR perfusion imaging of pulmonary parenchyma using pulsed arterial spin labeling techniques: FAIRER and FAIR. J Magn Reson Imaging 1999; 9: 483–87
104. Arai TJ, Prisk GK, Holverda S et al: Magnetic resonance imaging quantification of pulmonary perfusion using calibrated arterial spin labeling. J Vis Exp, 2011; (51). pii: 2712
105. Martirosian P, Boss A, Schraml C et al: Magnetic resonance perfusion imaging without contrast media. Eur J Nucl Med Mol Imaging, 2010; 37(Suppl.1): 52–64
106. Bolar DS, Levin DL, Hopkins SR et al: Quantification of regional pulmonary blood flow using ASL-FAIRER. Magn Reson Med, 2006; 55(6): 1308–17
107. Gaaß T, Dinkel J, Bauman G et al: Non-Contrast-Enhanced High Resolution MRI of the Pulmonary Blood Volume Using a Two Compartment Model and T1 Mapping. In: Proceedings of the 19th annual meeting of the ISMRM, Montreal, Canada, 2011; 4756
108. Deimling M, Jellus V, Geiger B et al: Time resolved lung ventilation imaging by Fourier decomposition. In: Proceedings of the Sixteenth Meeting of the International Society for Magnetic Resonance in Medicine. Berkeley, Calif: International Society for Magnetic Resonance in Medicine, 2008; 2639
109. Bauman G, Puderbach M, Deimling M et al: Non-contrast-enhanced perfusion and ventilation assessment of the human lung by means of fourier decomposition in proton MRI. Magn Reson Med, 2009; 62(3): 656–64
110. Chefd'hotel C, Hermosillo G, Faugeras O: Flows of Diffeomorphisms for Multimodal Image Registration. Proceedings of the IEEE International Symposium on Biomedical Imaging (ISBI'2002), Piscataway, NJ, USA: Institute of Electrical and Electronics Engineers: 753–56
111. Zapke M, Topf HG, Zenker M et al: Magnetic resonance lung function – a breakthrough for lung imaging and functional assessment? A phantom study and clinical trial. Respir Res, 2006; 6(7): 106
112. Suga K, Ogasawara N, Okada M et al: Lung perfusion impairments in pulmonary embolic and airway obstruction with noncontrast MR imaging. J Appl Physiol, 2002; 92(6): 2439–51
113. Bauman G, Lützen U, Ullrich M et al: Pulmonary functional imaging: qualitative comparison of Fourier decomposition MR imaging with SPECT/CT in porcine lung. Radiology, 2011; 260(2): 551–59
114. Bauman G, Eichinger M, Deimling M et al: Non-Contrast-Enhanced lung perfusion MRI in comparison to Contrast-Enhanced MRI perfusion in young cystic fibrosis patients. Am J Respir Crit Care Med, 2010; 181(1): A1828